Cell Calcium 79 (2019) 57–67

Contents lists available at ScienceDirect

Cell Calcium

journal homepage: www.elsevier.com/locate/ceca

A novel STIM1-Orai1 gating interface essential for CRAC channel activation

Carmen Butorac[a,1], Martin Muik[a,1], Isabella Derler[a], Michael Stadlbauer[a], Victoria Lunz[a], Adéla Krizova[a], Sonja Lindinger[a], Romana Schober[a], Irene Frischauf[a], Rajesh Bhardwaj[b], Matthias A. Hediger[b], Klaus Groschner[c], Christoph Romanin[a,*]

[a] Institute of Biophysics, Johannes Kepler University Linz, Gruberstrasse 40, 4020 Linz, Austria
[b] Institute of Biochemistry and Molecular Medicine, University of Bern, Buehlstrasse 28, CH-3012 Bern, Switzerland
[c] Gottfried Schatz Forschungszentrum, Medizinische Universität Graz, Neue Stiftingtalstraße 6, 8010 Graz, Austria

ARTICLE INFO

Keywords:
STIM1
Orai1
CRAC channel gating
Patch-clamp
Fluorescence microscopy

ABSTRACT

Calcium signalling through store-operated calcium (SOC) entry is of crucial importance for T-cell activation and the adaptive immune response. This entry occurs via the prototypic Ca^{2+} release-activated Ca^{2+} (CRAC) channel. STIM1, a key molecular component of this process, is located in the membrane of the endoplasmic reticulum (ER) and is initially activated upon Ca^{2+} store depletion. This activation signal is transmitted to the plasma membrane via a direct physical interaction that takes place between STIM1 and the highly Ca^{2+}-selective ion channel Orai1. The activation of STIM1 induces an extended cytosolic conformation. This, in turn, exposes the CAD/SOAR domain and leads to the formation of STIM1 oligomers. In this study, we focused on a small helical segment (STIM1 α3, aa 400–403), which is located within the CAD/SOAR domain. We determined this segment's specific functional role in terms of STIM1 activation and Orai1 gating. The STIM1 α3 domain appears not essential for STIM1 to interact with Orai1. Instead, it represents a key domain that conveys STIM1 interaction into Orai1 channel gating. The results of cysteine crosslinking experiments revealed the close proximity of STIM1 α3 to a region within Orai1, which was located at the cytosolic extension of transmembrane helix 3, forming a STIM1-Orai1 gating interface (SOGI). We suggest that the interplay between STIM1 α3 and Orai1 TM3 allows STIM1 coupling to be transmitted into physiological CRAC channel activation.

1. Introduction

Calcium signalling that occurs through store-operated calcium (SOC) entry is crucially important for T-cell activation and mast cell degranulation. The CRAC channel pathway is one of the most prominent calcium signalling routes. CRAC entry is initiated by the depletion of the endoplasmic reticulum (ER) calcium stores. This occurs when the second messenger molecule inositol-1,4,5-triphosphate (IP_3) binds to IP_3-receptors. In turn, this signal is transmitted to plasma membrane (PM) resident Ca^{2+} channels and promotes Ca^{2+} entry [1]. When the stromal interaction molecule 1 (STIM1) and Orai1 were identified as the main molecular components of this mechanism, a milestone was reached in the field of calcium signalling [2–8].

STIM1 represents the ER-located Ca^{2+} sensor, and Orai1 forms a highly Ca^{2+}-selective channel, which is located in the PM. In resting cells, STIM1 is uniformly distributed throughout the ER membrane and has a stable connection to microtubules [9,10]. Store depletion triggers the release of STIM1 from these cytoskeletal structures and its translocation into ER-PM junctions [11–13]. Once it has reached these junctions, STIM1 recruits Orai1 and a STIM1/Orai1 interaction occurred. This interaction leads to the formation of clusters at which local Ca^{2+} entry takes place [14–17]. This activation process involves ascertainable, mechanistic steps that include STIM1 homo-/oligomerization as well as conformational rearrangements within specific cytosolic domains [18–20]. The latter rearrangements are accompanied by the release and exposure of key regions (see Fig. 1), such as SOAR (STIM1-Orai1 activation region, aa 344–442) or CAD (CRAC activation domain, aa 342–448) which are indispensable for the STIM1-dependent activation of Orai1 channels. STIM1 binding to and communication with Orai1 are predominantly achieved via direct interactions with their C-terminal strands [15,21]. Stathopulos et al. subsequently characterized this heteromeric coiled-coil formation on a structural basis by employing STIM1/Orai1 C-terminal fragments. They found that the formation mainly involves the second coiled-coil domain (CC2) of STIM1

* Corresponding author.
E-mail address: christoph.romanin@jku.at (C. Romanin).
[1] These authors contributed equally.

https://doi.org/10.1016/j.ceca.2019.02.009
Received 5 February 2019; Received in revised form 19 February 2019; Accepted 20 February 2019
Available online 23 February 2019
0143-4160/ © 2019 The Authors. Published by Elsevier Ltd. This is an open access article under the CC BY-NC-ND license (http://creativecommons.org/licenses/BY-NC-ND/4.0/).

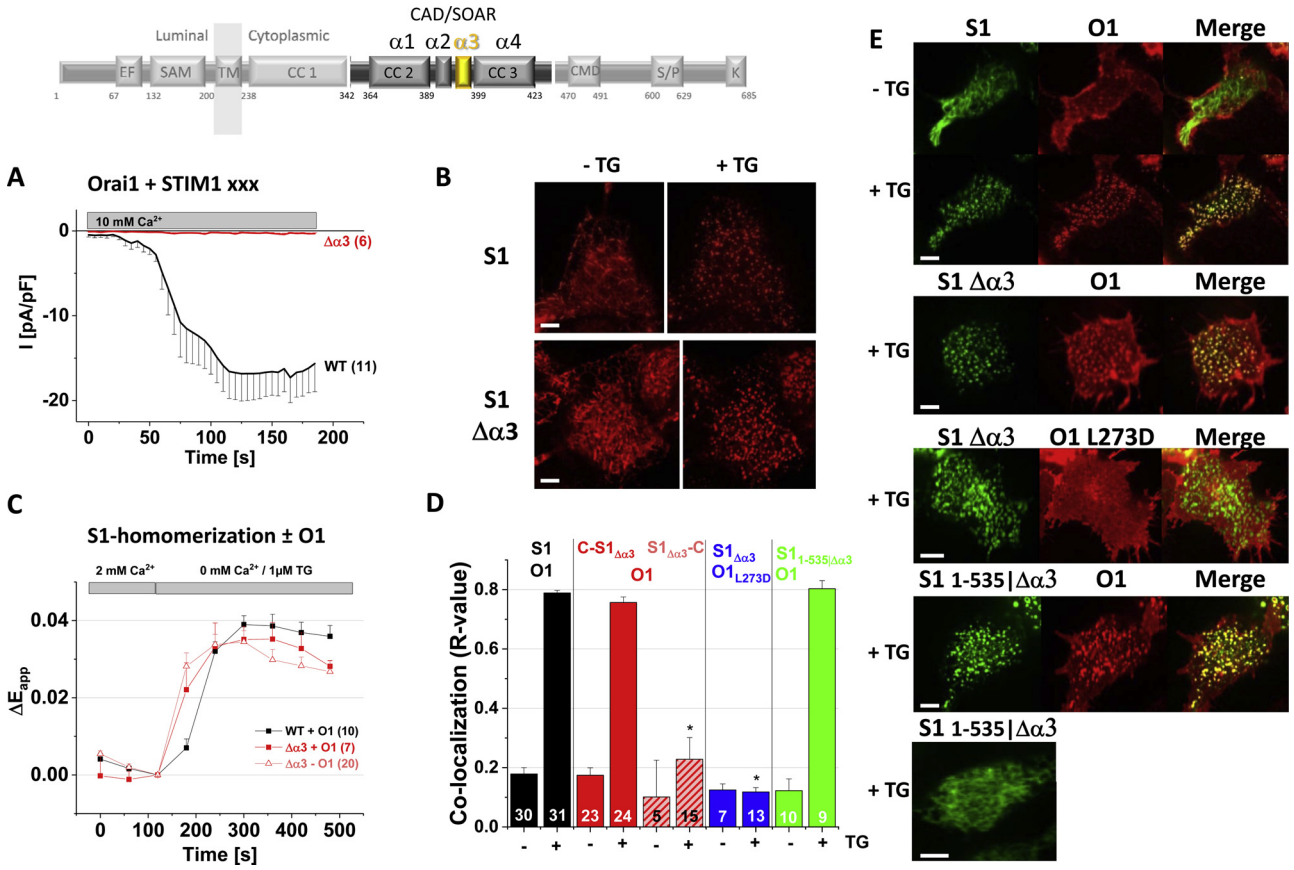

Fig. 1. The STIM1 α3 domain is necessary for Orai1 activation.
A time course of whole cell, inward currents at −74 mV, activated by passive store depletion of HEK293 cells expressing Orai1 WT together with either STIM1 WT or STIM1 Δα3 (Δaa400–403). *B* fluorescence images of Y-STIM1 WT and Y-STIM1 Δα3 before and after application of 1 μM TG. Lengths of scale bars correspond to 5 μm. *C* time course of FRET (E_{app}) monitoring the homomerization of the respective C/Y-labelled STIM1 constructs mentioned in *A* in response to 1 μM TG in the presence and absence of Orai1 WT. *D* calculated Pearson-coefficient (R-value) as a quantitative measurement of co-localization between the indicated C-STIM1 and Y-Orai1 mutants compared to WT before and after treatment with 1 μM TG. With STIM1 Δα3, co-localization of both the N-terminally (C-$S1_{Δα3}$) and the C-terminally ($S1_{Δα3}$-C) labelled forms are depicted. (number of cells are indicated within each bar). ***E*** fluorescence images of representative cells (CFP-green, YFP-red) after treatment with 1 μM TG as well as an overlay (merge) for visual comparison. Focused to the bottom section of the cell with a lengths of scale bars corresponding to 5 μm.

[22].

Although the binding of STIM1 to Orai1 C-terminus is an absolute premise, this does not seem to be sufficient for channel gating and the involvement of additional domains, such as the N-terminus and the cytosolic loop of Orai1, is still required [8,23–26]. Unlike the coupling of STIM1 CAD/SOAR to Orai1 C-terminus, much less is known about other regions within STIM1 that accomplish Orai1 gating [27].

In this study, we focus on the role of a small helical domain (i.e. alpha3) within STIM1 CAD/SOAR (see scheme in Fig. 1) that is crucial for Orai1 activation. This region is shown to contribute to the transmission of a gating signal from STIM1 to Orai1, as deletions or specific mutations therein result in abolished Orai1 currents. Interestingly, these STIM1 α3 mutants still bind to Orai1, but they fail to trigger Orai1 channel gating. The crosslinking of cysteines introduced in STIM1 α3 and the cytosolic Orai1 TM3 region resulted biochemically in the formation of a STIM1-Orai1 complex and in the stimulation of Orai1 channel currents. These results suggest that these regions are close to each other and are functionally essential for gating signal transmission. The results of the current study show that the SOGI formed between STIM1 α3 and Orai1 TM3 plays a crucial role in that it allows STIM1 binding to be relayed into Orai1 channel activation.

2. Results

2.1. The STIM1 α3 domain is necessary for Orai1 activation

To examine the role of the α3 region (aa 400–403) in STIM1 (see scheme in Fig. 1), we initially deleted the whole domain (STIM1 Δα3) to characterize its functional impact. This deletion fully abolished the capability of STIM1 to activate Orai1 currents (Fig. 1A). However, the propensity to form clusters was not affected, as STIM1 Δα3 was still able to form punctae in response to TG-induced store depletion when expressed without Orai1 (Fig. 1B). Homomerisation of STIM1 Δα3 both without and with Orai1 was only slightly reduced compared to that observed for STIM1 WT, as evaluated with FRET measurements (Fig. 1C),

Next, we examined whether STIM1 Δα3 was still able to couple to Orai1. Unfortunately, our initial attempts to perform FRET experiments were hampered. We hypothesized that this was due to the reduced affinity of STIM1 Δα3 to Orai1, which potentially originated from steric interference of the required C-terminal STIM1 Δα3 labelling. This hypothesis was supported by the observation that the co-localization of the C-terminally labelled STIM1 Δα3 with Orai1 was substantially reduced compared to the co-localization of the N-terminally labelled STIM1 Δα3 (Fig. 1D). Thus, we used the degrees of co-localization (Pearson coefficient) observed between the full-length N-terminally labelled STIM1 forms and Orai1 as semi-quantitative measures of their

coupling efficiencies.

STIM1 Δα3 and STIM1 WT co-localized equally with Orai1 (Fig. 1D, E). STIM1 Δα3 did not co-localize with Orai1 L273D, which was expected, as the introduction of this C-terminal point mutation has been shown to fully disrupt STIM1 binding to Orai1 [16,28](Fig. 1D, E). To further investigate the implications of the co-localization regarding the interactions between STIM1 forms and Orai1, we utilized a C-terminally shortened fragment of STIM1 ($STIM1_{1\text{-}535}$ Δα3) [29]. The fact that the polybasic cluster at the very end of the STIM1 C-terminus was specifically deleted prevented $STIM1_{1\text{-}535}$ Δα3 cluster formation in the absence of Orai1 (Fig. 1E, bottom row). In contrast, $STIM1_{1\text{-}535}$ Δα3 clearly showed the same degrees of co-localization and cluster formation with co-expressed Orai1 as STIM1 WT (Fig. 1D, E). These findings suggested that the overall interaction of N-terminally labelled, full-length STIM1 with Orai1 was not affected by the α3 domain deletion.

To further investigate the implications of co-localization, we used the smallest, Orai1-activating STIM1 fragment (i.e. a CAD/SOAR-like region (aa 344–449)) in an ER-tethered form to mimic the ER localization of a full-length STIM1 (Supp-Fig. 1A). To prevent steric interference, the fluorophore was luminally linked to the N-terminus in a construct (TMG-CAD) that we derived using our recently established FIRE-system [20]. Again, we observed that the degree of co-localization between TMG-CAD Δα3 and Orai1 was comparable to that seen with TMG-CAD WT (Supp-Fig. 1C, D), but TMG-CAD Δα3 failed to constitutively activate Orai1 currents (Supp-Fig. 1B). Taken together, these results demonstrated that STIM1 Δα3 exhibited homomerisation, punctae formation and specific co-localization with Orai1 upon store depletion to a similar extent as STIM1 WT. Our results also showed, however, that STIM1 Δα3 failed to induce CRAC currents, suggesting that STIM1 Δα3 was not able to effectively elicit Orai1 gating.

Because Orai1 activation was severely impacted when the whole STIM1 α3 helix was deleted, we subsequently deleted individual amino acids within this region (STIM1 Δ400, STIM1 Δ401, STIM1 Δ402, STIM1 Δ403, see scheme in Fig. 2). Every single amino acid deletion impaired Orai1 activation (Fig. 2A), despite the fact that each STIM1 mutant remained co-localized with Orai1 (Fig. 2B). These findings led us to investigate the potential impact of the helicity of the whole α3 region. It is known that the presence of poly-alanines favours, while poly-glycines weaken, the helical propensity [30]. For this reason, we first mutated the whole α3 region to alanines (STIM1 $_{400}AAAA_{403}$). We observed that the degree of co-localization with Orai1 and Orai1 activation were comparable to those seen with STIM1 WT (Fig. 2C, D). When we mutated the whole α3 region to glycines (STIM1 $_{400}GGGG_{403}$), however, Orai1 activation was completely abolished (Fig. 2C), although slightly diminished but still robust co-localization was observed (Fig. 2D).

These results suggested that the α3 region as a whole entity with its helical structure was required to elicit the STIM1-dependent gating of the Orai1 channel. We then conducted an additional aspartate screen within the alanine mutant (STIM1 $_{400}AAAA_{403}$). This revealed that all STIM1 mutants (STIM1 $_{400}DAAA_{403}$, STIM1 $_{400}ADAA_{403}$, STIM1 $_{400}AADA_{403}$, STIM1 $_{400}AAAD_{403}$) co-localized with Orai1 like STIM1 WT, regardless of the position of the aspartate within the α3 domain (Fig. 2D). Aspartates placed at positions 400, 401 and 403 did not interfere with Orai1 activation, though Orai1 currents obtained with STIM1 $_{400}DAAA_{403}$ as well as STIM1 $_{400}ADAA_{403}$ and STIM1 $_{400}AAAD_{403}$ were reduced and enhanced, respectively, compared to the currents obtained with STIM1 WT (Fig. 2C). Strikingly, STIM1 $_{400}AADA_{403}$, which had an aspartate at position 402, failed to activate Orai1 currents (Fig. 2C), despite the fact that the co-localization with Orai1 was retained (Fig. 2D).

These findings led us to more closely examine residue L402, and we subsequently substituted it with several different amino acids. We discovered that the store-operated currents for these mutants were comparable to those seen for STIM1 WT if small and uncharged amino acids were inserted at this position (STIM1 L402 A, STIM1 L402S) (Fig. 2E). If larger or positively charged residues were inserted (STIM1 L402Q, STIM1 L402 K), Orai1 was also activated, but to a lower extent than with STIM1 WT (Fig. 2E). The extent of co-localization with Orai1 for all these mutants was comparable to that seen with STIM1 WT or slightly reduced (Fig. 2F). Interestingly, when we introduced a negative charge at position 402 (STIM1 L402D, STIM1 L402E), we could abolish Orai1 activation, despite the fact that reduced but still pronounced co-localization was observed (Fig. 2E, F).

Our earlier attempt to use FRET as a complimentary approach to examine the extent of co-localization between Orai1 and full-length STIM1 α3 mutants had not been successful. For this reason, we used N-terminally labelled CAD/SOAR mutants (CAD Δα3, CAD L402D) instead and assessed these for their affinity to Orai1 by performing FRET and patch clamp measurements. In addition, we utilized 2-APB to promote an association between CAD forms and Orai1, as this method has been successfully established by Wang et al. [27]. We examined whether this association was accompanied by an additional increase in the potential transient current. These CAD α3 mutants exhibited a reduced affinity and FRET with Orai1 (Supp-Fig. 2A, B), but reached levels that were close to those of WT CAD upon application of 2-APB (Supp-Fig. 2A, B).

In the corresponding patch clamp experiments, CAD WT showed constitutive currents that were increased in a transient manner upon 2-APB application, as expected (Supp-Fig. 2C, D). However, no constitutive currents were evoked with the CAD α3 mutants, and only minor current enhancements were observed following the application of 2-APB (Supp-Fig. 2C, D). These minor functional responses were divergent from the pronounced increases observed in the affinity and FRET of these mutants to Orai1. Consistent electrophysiological results were obtained for full-length STIM1 WT and the STIM1 α3 mutants following 2-APB application. Only minor current enhancements were observed for the gating-deficient STIM1 α3 mutants, while large transient current increases were observed with STIM1 WT (Supp-Fig. 2E, F). Taken together, these results suggested that the STIM1 α3 region moderately affected the affinity between STIM1 and Orai1, but still represented a key domain in the process that led to Orai1 channel gating.

2.2. Partially open Orai1 P245L restores the gating propensity of STIM1 α3 mutants

Next, we tested whether the constitutively active Orai1 P245L mutant [31–34] could compensate for the gating defect related to the Orai1 channel activation process observed for the STIM1 α3 mutants. We assumed that Orai1 P245L was already constitutively active and that a partially open state existed upon starting whole-cell recording. This constitutive activity was further enhanced following store depletion in a STIM1-dependent manner (Fig. 3A). We consistently observed that the additional current enhancement was strictly dependent on the coupling between STIM1 and Orai1 P245L (Fig. 3B, C). The increase in both the current and extent of co-localization was abolished upon the mutational disruption of the main STIM1 binding site on the Orai1 C-terminus, i.e. Orai1 L273D (Fig. 3A–C).

The co-expression of Orai1 P245L with either of the gating-deficient STIM1 α3 mutants also resulted in the activation of Orai1 P245L currents following store-depletion (Fig. 3D, G) to the same level seen for STIM1 WT (Fig. 3A). This co-expression was accompanied by an extent of co-localization for STIM1 Δα3 that was comparable to that of Orai1 WT (Fig. 3E, F) and was slightly higher than that of STIM1 L402D (Fig. 3F, H). The I/V-relationship of both mutants displayed a characteristic, strong inward rectification with a reversal potential > + 50 mV, which was comparable to that seen for STIM1 WT-induced currents (Fig. 3I). We assumed that the regain of Orai1 P245L gating observed for the STIM1 α3 mutants was the result of a mechanism that was distinct from one that was recently reported [35] for the non-functional STIM1 F394H and R429C mutants. These mutants failed to

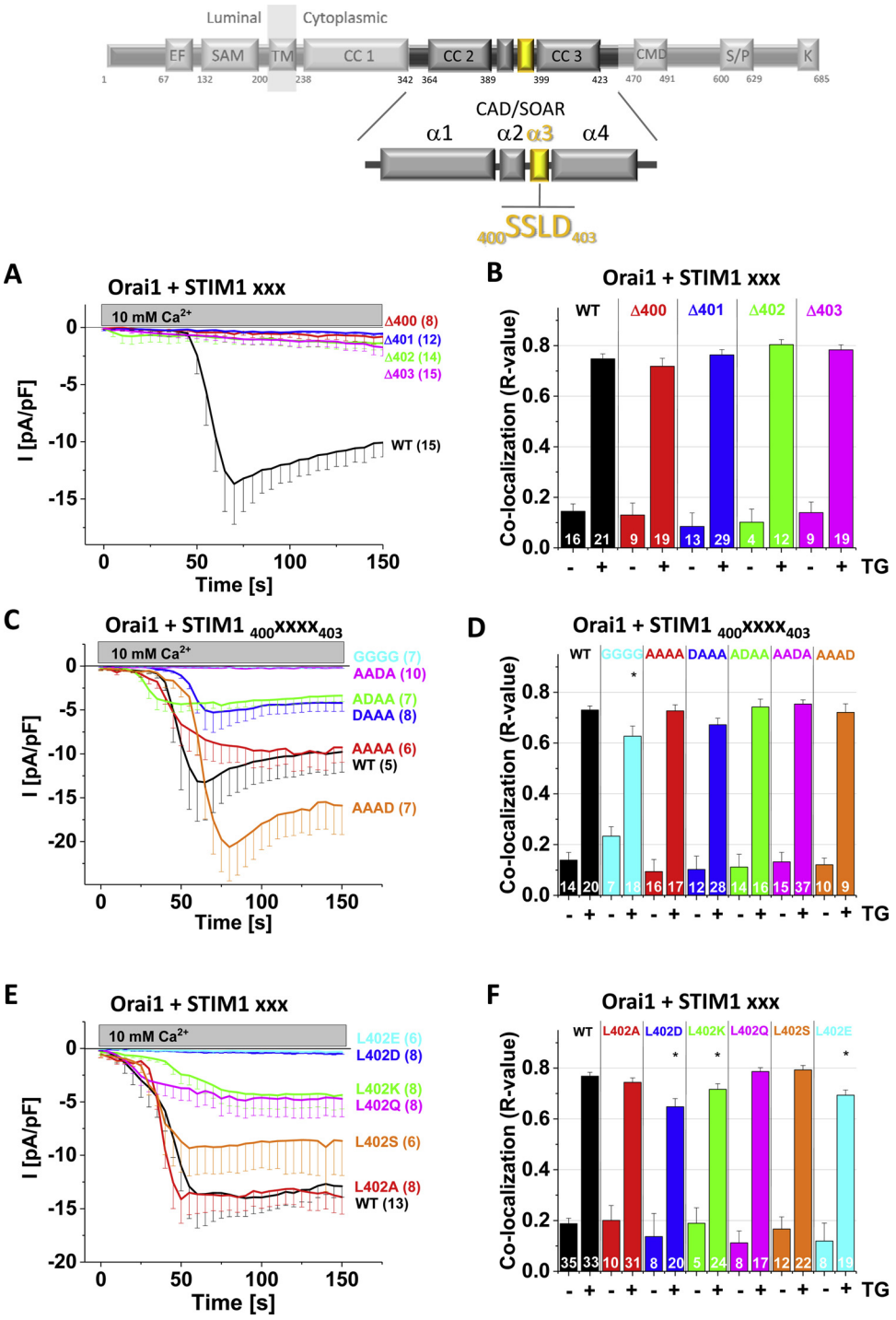

Fig. 2. Mutational screen in STIM1 α3.
A time course of whole cell inward currents at −74 mV activated by passive store depletion of HEK293 cells, expressing Orai1 WT together with either STIM1 WT or STIM1 α3 single deletion mutants. *B* calculated Pearson-coefficient (R-value) as a quantitative measurement of co-localization for the constructs measured in *A* before and after treatment with 1 μM TG (number of cells are indicated within each bar). *C* time course of whole-cell, inward currents at −74 mV, activated by passive store depletion of HEK293 cells expressing Orai1 WT together with either STIM1 WT or STIM1 α3 multiple-point mutants. *D* calculated Pearson-coefficient (R-value) as a quantitative measurement of co-localization for the constructs measured in *C* before and after treatment with 1 μM TG (number of cells are indicated within each bar). ***E*** time course of whole-cell, inward currents at −74 mV, activated by passive store depletion of HEK293 cells expressing Orai1 WT together with either STIM1 WT or STIM1 L402 mutants. ***F*** calculated Pearson-coefficient (R-value) as a quantitative measurement of co-localization for the constructs measured in *E* before and after treatment with 1 μM TG (number of cells are indicated within each bar).

co-localize with and activate Orai1 WT, but the activation could be restored by the Orai1 P245L mutation, primarily due to an increase in the mutant STIM1 binding to Orai1 P245 L [35]. These findings were corroborated by the discovery that Orai1 P245L has a higher affinity towards STIM1, revealed by the results of localization experiments in which the STIM1 C-terminus was utilized as a cytosolic fragment in Orai1 or Orai1 P245L co-expressing cells (Supp-Fig. 4A, B). We did not believe that the gating propensity of the STIM1 α3 mutants was restored by the small increase in their affinity with Orai1 P245L, as suggested from the slight increase in co-localization of STIM1 α3 mutants and Orai1 P245L when compared to Orai1 WT (Fig. 3E, H). Instead, we hypothesized that the constitutively active Orai1 P245L channel mutant provides a trigger signal that allows the transmission of STIM1 coupling into gating of the Orai1 WT channels, and this signal is lacking in the STIM1 α3 mutants.

2.3. Orai1 E173K restores the gating deficiency of STIM1 α3 mutants

Data recently published by Zhou et al. [36] suggest that the hinge region in TM4 and the C-terminal cytosolic helical extension of TM4 (TM4-ext) of Orai1, as well as the neighbouring TM3, play key roles in the Orai1 channel activation process. The main interaction with STIM1 is mediated by the Orai1 C-terminus [15,37]. The degree of co-localization indicated that this interaction was similar for STIM1 WT and STIM1 α3 mutants. Hence, we hypothesized that the lack of Orai1 gating observed in STIM1 α3 mutants could be due to an impairment in

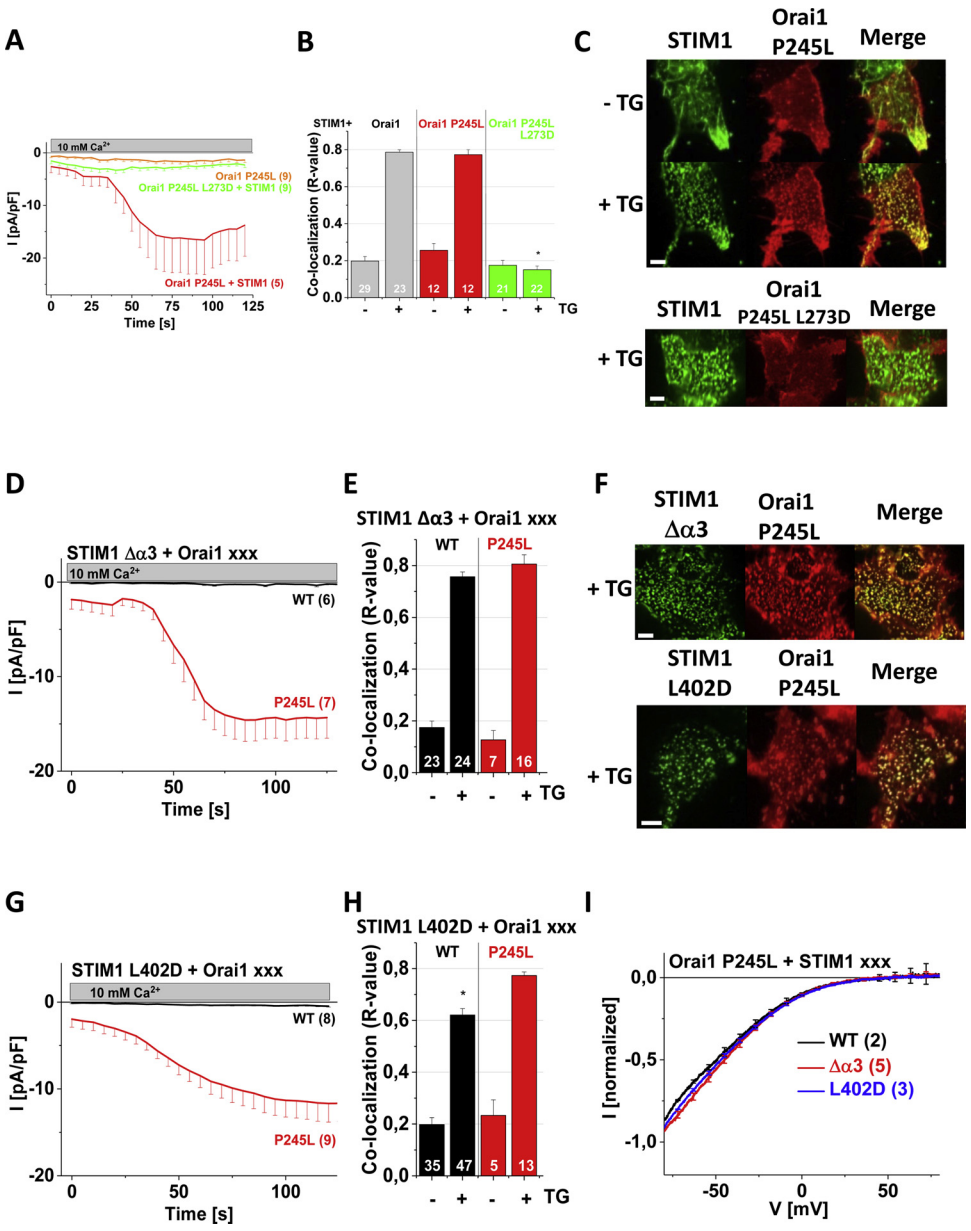

Fig. 3. Partially open Orai1 P245 L restores gating propensity of STIM1 α3 mutants.
A time course of whole-cell, inward currents at −74 mV, activated by passive store depletion of HEK293 cells expressing Orai1 P245L as well as Orai1 P245L L273D together with STIM1 WT. Orai1 P245L alone is shown as a control (orange). *B* calculated Pearson-coefficient (R-value) as a quantitative measurement of co-localization between the indicated Y-Orai1 mutants and C-STIM1 WT. Orai1 WT (grey) was taken as a control. ***C*** corresponding fluorescence images for visual comparison. Focused to the bottom section of the cell with a lengths of scale bars corresponding to 5 µm. *D* time course of whole-cell, inward currents at −74 mV, activated by passive store depletion of HEK293 cells expressing STIM1 Δα3 together with either Orai1 WT (black) or Orai1 P245L (red). *E* co-localization corresponding to measurements in *D* (number of cells are indicated within each bar). *F* fluorescence images corresponding to measurements in *E* and *H*. Focused to the bottom section of the cell with a lengths of scale bars corresponding to 5 µm. ***G*** time course of whole-cell, inward currents at −74 mV, activated by passive store depletion of HEK293 cells expressing STIM1 L402D together with either Orai1 WT (black) or Orai1 P245 L (red). *H* co-localization corresponding to measurements in *G* (number of cells are indicated within each bar). ***I*** I/V relationship of Orai1 P245L co-expressed with either STIM1 WT, STIM1 Δα3 or STIM1 L402D.

the transmission of STIM1 coupling into Orai1 gating via TM3. Here, the presence of the STIM1 α3 domain might support the gating signal relay from Orai1 TM4/TM4-ext to TM3 L174 [36].

To test this hypothesis experimentally, we first engineered Orai1 TM3 L174 K and TM3 L174D mutants and examined their potential activation with both STIM1 WT and STIM1 α3 mutants. These forms of STIM1 were not able to activate Orai1 L174 K or Orai1 L174D (Fig. 4A, Supp-Fig. 3B). These results are consistent with a general, profound block of STIM1-induced Orai1 activation reported in [38]. Next, we extended the search to the more upstream cytosolic portion of Orai1 TM3 (residues 166–173, see Supp-Fig. 3A) in an attempt to rescue the Orai1 function in the presence of STIM1 Δα3 and STIM1 L402D. We initially mutated residue E166, which is located closest to the cytosol and points toward the TM4-ext (Supp-Fig. 3A) (E166Q, E166 K), and residue E173, which is adjacent to L174 (E173Q and E173K). These Orai1 mutants were still activated by STIM1 WT (Supp-Fig. 3C, *left panel*) and exhibited degrees of co-localization that were comparable to that with Orai1 WT (Supp-Fig. 3D, left panel). When co-expressed with STIM1 L402D, these Orai1 mutants revealed a substantial degree of co-localization (Supp-Fig. 3D, right panel), and Orai1 E166Q – but not Orai1 E166K – and Orai1 E173Q yielded extremely small store-operated currents. Strikingly, only Orai1 E173K was substantially activated by STIM1 L402D in a store-dependent manner (Supp-Fig. 3C, *right panel*). Moreover, both STIM1 Δα3 and STIM1 L402D showed clear store-dependent activations of Orai1 E173K currents, although these were observed to a lower extent as compared with STIM1 WT (Fig. 4B). These currents also exhibited strong inward rectification and a reversal potential that was similar to those obtained with STIM1 WT (Fig. 4C). As both α3 mutants showed degrees of co-localization with Orai1 E173K (Fig. 4D, E) that were comparable to that observed with Orai1 WT (Figs. 1D, 2 F), we concluded that the activation of the Orai1 E173K current was not due to an increase in the affinity to the STIM1 forms. The STIM1 C-terminus consistently showed a similar affinity to Orai1 E173K and Orai1 WT (Supp-Fig. 4C, D). Overall, these experiments suggested that Orai1 E173K apparently provided part of the gating signal which is usually provided by the STIM1 α3 domain.

2.4. Close proximity of STIM1 α3 and Orai1 TM3

The results reported in the previous section suggest that an interplay

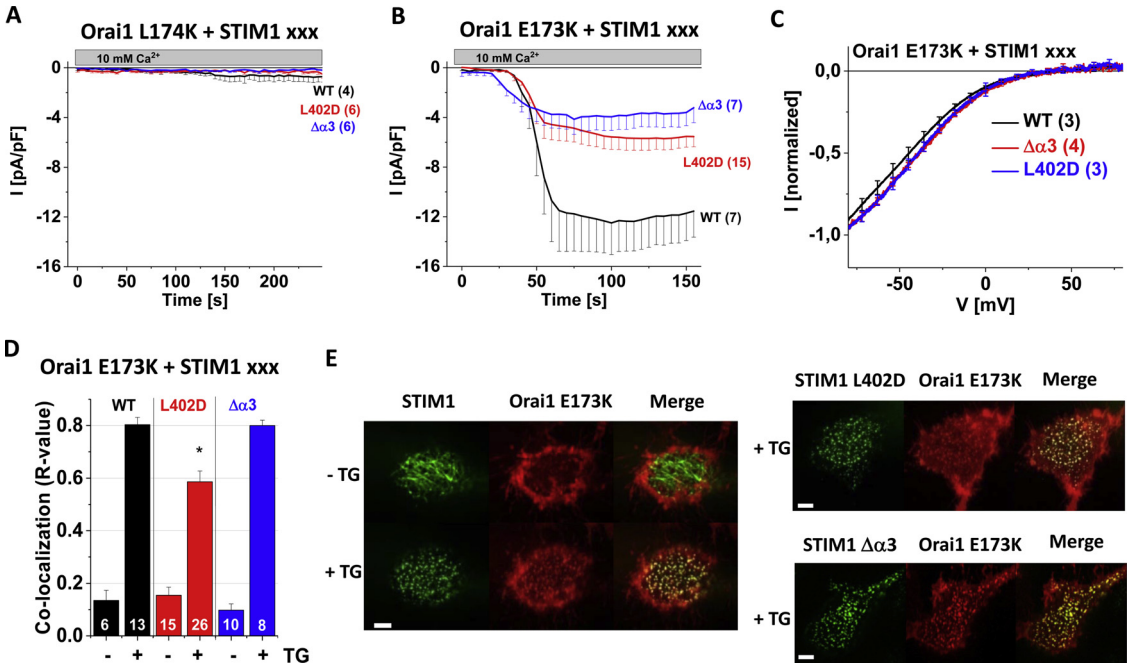

Fig. 4. Orai1 E173K restores the gating defieciency of STIM1 α3 mutants.
A time course of whole-cell, inward currents at −74 mV, activated by passive store depletion of HEK293 cells expressing Orai1 L174K together with STIM1 WT, STIM1 L402D, or STIM1 Δα3. *B* time course of whole-cell, inward currents at −74 mV, activated by passive store depletion of HEK293 cells expressing Orai1 E173K together with STIM1 WT/STIM1 Δα3/STIM1 L402D. *C* I/V relationship of measurements in *B*. *D* co-localization corresponding to measurements in *B*. *E* corresponding fluorescence images for visual comparison. Focused to the bottom section of the cell with a lengths of scale bars corresponding to 5 µm.

occurs between STIM1 α3 and Orai1 TM3 which is necessary for Orai1 channel opening. To identify the STIM1 α3 target site on Orai1 TM3, we carried out cysteine crosslinking experiments to determine whether these two domains were close to each other. Taking a straightforward approach, we mutated STIM1 L402 and a potential interaction partner at the cytosolic end of TM3 (E162, E166, R170, E173; see Fig. 5A) to a cysteine. To prevent the involvement of other endogenous cysteines in STIM1/Orai1, we also mutated a potentially interfering cysteine residue that was located in the C-terminus of STIM1 (C437S), and we created an Orai1 variant that lacked all three endogenous cysteines (Orai1 C126V C143V C195V: $Orai1_{cys\text{-}free}$). In line with earlier studies of [39], we found that the co-expression of $Orai1_{cys\text{-}free}$ and STIM1 WT yielded only very low currents (Supp-Fig. 5E). The currents obtained for $Orai1_{cys\text{-}free}$ and STIM1 C437S were similar in size and did not alter when the cysteine-crosslinking reagent diamide was added (Supp-Fig. 5F).

We observed a robust co-localization with STIM1 L402C C437S for all $Orai1_{cys\text{-}free}$ TM3 mutant forms following store depletion, although the degree of co-localization was somewhat elevated in some of these $Orai1_{cys\text{-}free}$ TM3 forms before store depletion (Fig. 5B). We conducted patch-clamp recordings of the $Orai1_{cys\text{-}free}$ TM3 mutants, revealing small, store-dependent, inward currents that were similar to those seen with $Orai1_{cys\text{-}free}$ activated by STIM1 L402C C437S (Fig. 5C). When diamide was applied in an attempt to potentially crosslink the respective cysteine residue of Orai1 TM3 with STIM1 L402C, we noted that the current only increased in the case of $Orai1_{cys\text{-}free}$ E166C, while the remaining mutants (E162C, R170C, E173C) collectively failed to show enhanced responses (Fig. 5C). The I/V-relationship of the diamide-induced currents displayed strong inward rectification with a reversal potential of around + 50 mV (Supp-Fig. 5B). When taking a biochemical approach, the results of cysteine crosslinking experiments with store-depleted HEK293 STIM1/Orai1 double knockout cells, analysed using a STIM1/Orai1 western blot, revealed complex formations between expressed $Orai1_{cys\text{-}free}$ E166C and STIM1 L402C C437S proteins upon treatment with diamide. These findings suggested a close proximity between STIM1 α3 and Orai1 TM3 (Fig. 5D, Supp-Fig. 6A). The additional band was observed only when STIM1 L402C C437S and $Orai1_{cys\text{-}free}$ E166C were co-expressed and diamide treatment was performed. These bands were exactly the same sizes on Orai1- and STIM1-antibody-detected blots (Fig. 5D and Supp-Fig. 6A), respectively.

This recognition by both Orai1- and STIM1-specific antibodies indicated that both proteins were present in a covalently linked STIM1-Orai1 complex. The molecular weight of the complex (between 200 and 250 kDa) did not allow us to deduce its stoichiometry, as it neither matched that of 1 STIM1/1 Orai1 (˜160 kDa), nor 2 STIM1/1 Orai1 (˜260 kDa). We suspected this was due to an anomalous migration behaviour [40] of the covalently linked STIM1-Orai1 complex. Furthermore, the diamide-induced Ca^{2+} current increase observed in patch-clamp recordings made with $Orai1_{cys\text{-}free}$ E166C and STIM1 L402C C473S was fully reversible upon the application of bis(2-mercaptoethyl) sulfone (BMS). This reagent is known to disrupt cysteine crosslinking (Fig. 5C insert, Supp-Fig. 5C). This reversibility was also verified by the results of Western blots, using the diamide-treated samples, upon the addition of BMS (Supp-Fig. 6B).

To exclude the possibility that the current enhancement observed with $Orai1_{cys\text{-}free}$ E166C was caused by crosslinking between neighbouring Orai1 subunits, we co-expressed this mutant together with STIM1 C437S instead of STIM1 L402C C437S. The addition of diamide did not result in a significant increase in the Ca^{2+} currents (Supp-Fig. 5D), which provided supportive evidence. In a second approach, we additionally mutated all other residues in STIM1 α3 to a cysteine (STIM1 S400C C437S, STIM1 S401C C437S, STIM1 D403C C437S). We then co-expressed each of these mutants with $Orai1_{cys\text{-}free}$ E166C. The extent of co-localization seen with $Orai1_{cys\text{-}free}$ E166C was only slightly lower for L401C and D403C and similar to that seen for the S400C or L402C STIM1 C437S mutants (Fig. 5E). One interesting result was that only STIM1 L402C C437S displayed current enhancement upon the application of diamide (Fig. 5F). Overall, these functional and biochemical data provided compelling evidence, allowing us to conclude that STIM1 α3 and Orai1 TM3 are close to one another. These data also suggest that an interface exists between these two domains or nearby residues, i.e. SOGI, that allows the transmission of STIM1 coupling into Orai1 channel gating.

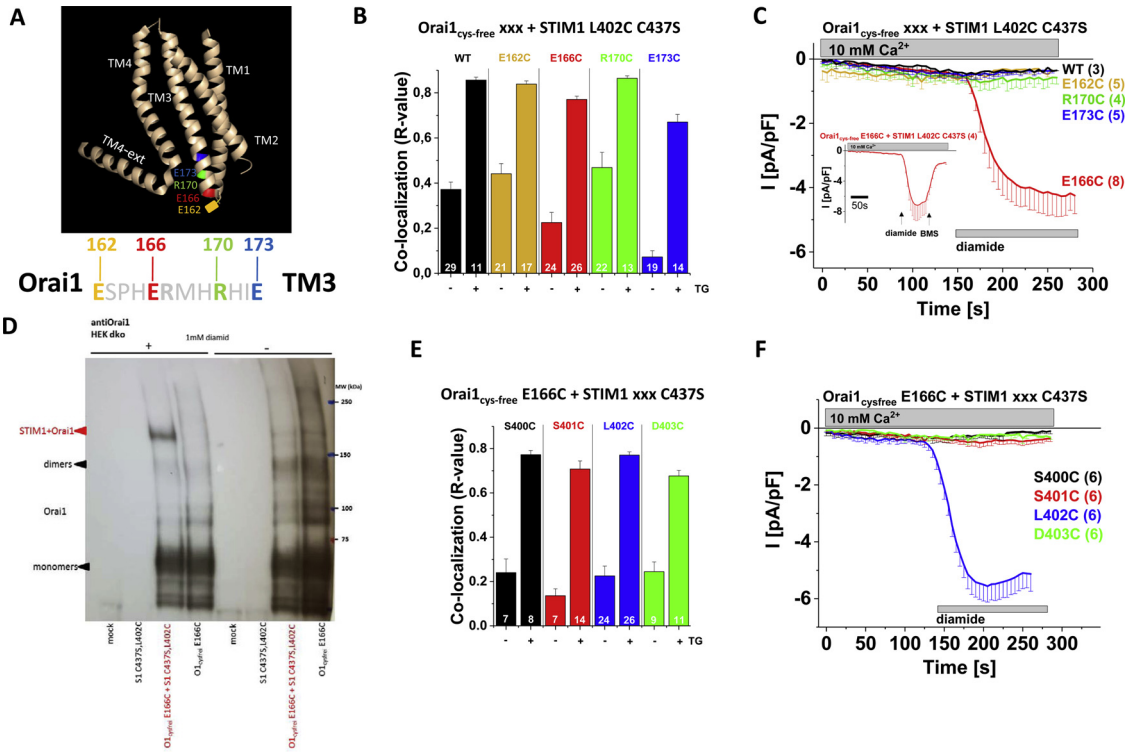

Fig. 5. Close proximity of STIM1 α3 and Orai1 TM3.
A model of dOrai generated via PyMOL. Amino acids within the cytosolic TM3 region, which are putative candidates for crosslinking with STIM1 L402C are highlighted in different colours. *B* calculated Pearson-coefficient (R-value) as a quantitative measurement of co-localization between the indicated Orai1 mutants and STIM1 L402C C437S before and after treatment with 1 μM TG (number of cells are indicated within each bar). *C* time course of whole-cell, inward currents at −74 mV, activated by passive store depletion of HEK293 cells expressing STIM1 L402C C437S together with the following $Orai1_{cys\text{-}free}$ mutants: WT (black), E162C (orange), E166C (red), R170C (green) and E173C (blue), the time point of diamide application is indicated by the bar. The insert shows the reversibility of the diamide induced crosslinking by application of BMS as indicated by the arrow. *D* representative Western Blot of crosslinking experiments overexpressing YFP or CFP labelled Orai1 and/or STIM1 constructs in STIM1/Orai1 double knockout HEK293 cells detected with an antiOrai1 antibody. Upon store-depletion with TG, samples were treated without or with 1 mM diamide. Bands at ~60 kDa correspond to Orai1 monomers. Bands at ~120 kDa correspond to Orai1 dimers. A STIM1-Orai1 aggregate can only be seen in STIM1 L402C C437S/$Orai1_{cys\text{-}free}$ E166C co-expressed, diamide-treated samples. Experiments were repeated at least 3 times with individual transfections. *E* calculated Pearson-coefficient (R-value) as a quantitative measurement of co-localization between $Orai1_{cys\text{-}free}$ E166C and the indicated STIM1 mutants before and after treatment with 1 μM TG (number of cells are indicated within each bar). ***F*** time course of whole-cell, inward currents at −74 mV, activated by passive store depletion of HEK293 cells expressing $Orai1_{cys\text{-}free}$ E166C and STIM1 L402C C437S. The reversibility of the diamide effect is shown by application of BMS as indicated by the bars.

3. Discussion

Our study on the small helical domain (α3) within the CAD/SOAR region of STIM1 reveal its major impact on the activation of store-operated Ca^{2+} entry. We identified the specific, functional role of STIM1 α3 in CRAC channel activation by deleting or individually mutating residues within this domain. The results show that STIM1 α3 is a discrete domain that plays a key role in relaying STIM1 coupling into Orai1 channel opening. Cysteine crosslinking of STIM1 with Orai1 functionally resulted in Ca^{2+} current enhancement. This crosslinking could be biochemically visualized in the formation of a STIM1/Orai1 complex by Western blotting, pointing to the fact that the cytosolic part of the Orai1 TM3 region might be a target site for STIM1 α3. Overall, this observed close proximity between STIM1 α3 and Orai1 TM3 suggests the presence of a STIM1-Orai1 gating interface (SOGI) that facilitates Orai1 channel gating upon STIM1 coupling.

The STIM1 α3 domain does not play a dominant role in store-depletion-induced STIM1 homomerisation and co-clustering with Orai1, both of which are prerequisites for Orai1 activation by STIM1. When co-expressed with Orai1, the degree of homomerisation of STIM1 Δα3 was comparable to that seen for STIM1 WT. Although the affinity for STIM1 Δα3 to Orai1 was slightly reduced, the perturbance was not as dominant as that seen for a previously reported STIM1 mutation within the upstream α2 region (i.e. STIM1 F394 H) [27]. Despite the fact that the features of STIM1 activation were preserved, Orai1 activation was abolished with STIM1 Δα3, indicating that the STIM1 α3 domain, in a direct or indirect manner, influenced the transmission of a gating signal that affects Orai1 channel opening.

We conducted a mutational screen, deleting each individual residue within the α3 region. This allowed us to identify fully or almost fully gating-deficient STIM1 deletion mutants that retained extents of co-localization with Orai1 that were similar to that seen for STIM1 WT. When we substituted the whole α3 region to alanines (STIM1 $_{400}AAAA_{403}$), no effect on the co-localization with Orai1 was observed; current levels that were similar to that seen with STIM1 WT were also seen. However, when we mutated the whole α3 region to glycines (STIM1 $_{400}GGGG_{403}$), thereby weakening the helical structure, we abolished channel activation despite the fact that the extent of co-localization with Orai1 was only slightly diminished.

Taken together, these results suggest that the α3 region – as a whole entity with the inherent helical structure – is essential for gating signal transmission within the Orai1 channel. Based on these results, we cannot exclude the possibility that the STIM1 α3 region has an indirect, allosteric effect. Nonetheless, we identified position 402 (STIM1 $_{400}AADA_{403}$) by conducting an aspartate screen within STIM1 $_{400}AAAA_{403}$ as the most effective one. This position was similar to STIM1 Δα3 in that it interfered with the activation of Orai1 without strongly affecting the extent of co-localization. An additional screen at

position 402 within STIM1 α3 revealed that specifically substituting the native amino acid at this position with negatively charged amino acids (D, E) fully abolished Orai1 channel activation but led to only a slight, yet significant, reduction in the extent of co-localization with Orai1.

This decrease in affinity became even more apparent when we created CAD α3 mutants that exhibited reduced levels of affinity as well as reduced FRET with Orai1. When we utilized 2-APB [27] to substantially restore the affinity and FRET with the gating-deficient STIM1 α3 mutants (STIM1 L402D, STIM1 Δα3), we observed only minor current enhancements. These significantly differed from the huge, transient current increases obtained when WT STIM1 or STIM1 F394H were used [27]. The latter STIM1 F394H mutant has been reported as unable to bind to or activate Orai1, but both its affinity to and activation of Orai1 can be restored by adding 2-APB. We could restore this affinity in our mutants, and especially our CAD α3 mutants, by adding 2-APB as well, but could not (or only to a minor extent) restore the activation of Orai1, showing that the α3 domain is necessary to elicit Orai1 gating.

We carefully examined the results of the detailed mutational screen, focusing on the STIM1 Δα3 and STIM1 L402D mutants to characterize their gating defects in more detail. We utilized the partially open Orai1 P245L channel mutant as a tool to determine whether the defect in gating was caused by deletion of α3 or whether the L402D mutation therein had a more severe, inhibitory impact on STIM1. Since both STIM1 α3 mutants were able to elicit store-dependent inward currents with Orai1 P245L in a manner similar to STIM1 WT, this suggested the presence of a functional deficiency that allowed the transmission of STIM1 binding into the Orai1 WT pore opening rather than a deficiency in the initial binding process itself.

We then proposed that the P245L mutation could allow for a higher affinity of STIM1 binding and observed a higher affinity of binding between the STIM1 C-terminus and Orai1 P245L. The degree of co-localization of STIM1 α3 mutants, and in particular of the L402D mutant, with Orai1 P245L was indeed slightly higher than that seen for Orai1 WT, but was comparable and equal to that of STIM1 WT. For this reason, we considered it more likely that Orai1 P245L was able to compensate for the lack of a gating trigger signal in STIM1 α3 mutants, allowing them to transmit their coupling into Orai1 gating. It is tempting to speculate that the Orai1 P245L mutation may have an impact on the TM4/TM4-ext region, which has been proposed to hydrophobically link the TM4 nexus region to the adjacent TM3, thus affecting the signal propagation towards TM1 and eliciting pore opening [36]. In the case of Orai1 WT, the TM3 or at least a certain region within TM3 could represent an acceptor site for STIM1 α3.

We tested this hypothesis initially by conducting a mutational screen within the more cytosolic portion of Orai1 TM3 to examine its impact on the STIM1-gating-deficient α3 mutants. We were indeed able to identify the Orai1 E173K mutant that substantially restored the activity of either gating-deficient STIM1 α3 mutant, although not to the full extent as seen for STIM1 WT. Unlike Orai1 P245L, the overall affinity of the STIM1 C-terminus to Orai1 E173K was comparable to its affinity to Orai1 WT. These results are in line with the extents of co-localization seen for STIM1 α3 mutants, which showed similarly high levels with either Orai1 WT or Orai1 E173K. Thus, it seemed as though Orai1 E173K provided part of the transmitting signal input that was otherwise provided by the STIM1 α3 domain. This residue is adjacent to L174 in Orai1 TM3, which plays a role in TM3/TM4 signal propagation [36]. Its mutation severely interferes with STIM1-dependent activation. As the activation levels of Orai1 WT or Orai1 E173K currents induced by STIM1 WT did not exhibit significant differences, we cannot infer that residue E173 in Orai1 itself represents a specific acceptor site for STIM1 α3. Moreover, the Orai1 residues upstream E173 in TM3 are considered to be more accessible to STIM1 when it approaches from the cytosolic side [41].

In an attempt to specifically identify the proximity between STIM1 α3 and Orai1 TM3, we carried out cysteine crosslinking studies with STIM1/Orai1 mutants that were devoid of endogenous cysteines and expressed them in a HEK293 STIM1/Orai1 double-knockout cell line. The results of these experiments revealed a close proximity between STIM1 L402C and E166C in the Orai1 cytosolic TM3. This proximity allowed biochemically for the formation of a STIM1/Orai1 complex and resulted functionally in a substantial Ca^{2+} current increase upon application of diamide. We are well aware of the fact that the introduction of cysteines may induce non-physiological interactions. Nonetheless, a number of studies have been carried out in the STIM/Orai field in which such experiments have been successfully used to obtain further structural information on close proximity (Orai pore: McNally et al., PNAS, 2009; Zhou et al, PNAS 2010; Orai1 TM3/TM4 nexus: Zhou et al., Nat Comm, 2016; STIM1 activation: Hirve et al, Cell Rep, 2018).

We have recently reported [42] that a decrease in currents observed in cysteine crosslinking studies on Orai1 K78C E166C suggests that a communication pathway exists between K78 in TM1 and E166 in TM3. This somewhat inhibitory communication might be released by the enforced engagement of E166C in Orai1 with L402C in STIM1. Recently, the structure of the constitutively active *Drosophila* Orai H206 A (equivalent to H134 A in human Orai1) [43] mutant was reported [44]. This structure suggests an unlatching of TM4 and between TM4 and TM3 as prerequisites to open the pore and expose cytosolic docking sites for STIM1. Based on our results, we propose that the Orai1 cytosolic TM3 stretch (between E173 and E166) is involved in the formation of a STIM1 Orai1 gating interface (SOGI) that relays a molecular trigger from the STIM1 α3 domain to elicit CRAC channel gating. As we cannot fully exclude that STIM1 alpha3 might serve as a passive structural component rather than as a direct actor in positioning a different surface of STIM1 for signal transmission to Orai1, our hypothesis of SOGI as physiological contact site awaits further proof once the STIM1/Orai1 complex has been structurally resolved.

4. Experimental procedures

4.1. Molecular cloning and mutagenesis

Human Orai1 (Orai1; accession no. NM_032790) was provided by A. Rao's Laboratory, Harvard Medical School. N-terminally tagged Orai1 constructs were cloned with SalI and SmaI restriction sites of pECFP-C1 and pEYFP-C1 expression vectors (Clontech). Orai1 mutants (P245 L, P245 L L273D, E166Q, E166 K, E173Q, E173 K, C126 V C143 V C195 V (cys-free), cys-free E166C, cys-free E162C, cys-free R170C, cys-free E173C) were generated using the QuikChange XL site-directed mutagenesis kit (Stratagene).

Human STIM1 (STIM1; accession no. NM_003156) N-terminally tagged with enhanced CFP (ECFP) and enhanced yellow fluorescent protein (EYFP) was provided by T. Meyer's Laboratory, Stanford University. STIM1 C terminus (amino acids 233–685) was cloned into the T/A site of pcDNA3.1V5 His TOPO by PCR and subcloned into pECFP-C1 and pEYFP-C1 via their internal restriction sites KpnI and XbaI. Construct for the FIRE system consists of STIM1-signal peptide, EYFP (Y), 29-aa linker, STIM1 transmembrane domain, 32-glycine linker followed by the protein fragment of interest (CAD 344–449). STIM1 mutants (L402D, Δ400-403, Δ400, Δ401, Δ402, Δ403, L402A, L402K, L402Q, L402S, L402E, $_{400}$AAAA$_{403}$, $_{400}$DAAA$_{403}$, $_{400}$ADAA$_{403}$, $_{400}$AADA$_{403}$, $_{400}$AAAD$_{403}$, $_{400}$GGGG$_{403}$, C437S, L402C C437S, S400C C437S, S401C C437S, D403C C437S) were generated using the QuikChange XL site-directed mutagenesis kit (Stratagene). The integrity of all resulting clones was confirmed by sequence analysis.

4.2. Cell culture and transfection

Human embryonic kidney 293 (HEK293) cells were cultured in DMEM supplemented with L-glutamine (2 mM), streptomycin (100 μg/ml), penicillin (100 units/ml) and 10% foetal calf serum at 37 °C in a humidity-controlled incubator with 5% CO_2. Transient transfection of

HEK293 cells was performed using the TransFectin Lipid Reagent (Bio-Rad). Measurements were carried out 24 h following transfection.

4.3. Generation of STIM1/Orai1 double knockout HEK293 cells using CRISPR/Cas9 genome editing

The guide RNA pairs within exon 1 of STIM1 were identified using the Benchling CRISPR webtool (https://benchling.com/crispr) and the following complementary oligos with BbsI compatible overhangs were designed:

STIM1_gRNA1 for: 5′-CAC CGT TCT GTG CCC GCG GAG ACT C-3′
STIM1_gRNA1 rev: 5′-AAA CGA GTC TCC GCG GGC ACA GAA C-3′
STIM1_gRNA2 for: 5′-CAC CGT ATG CGT CCG TCT TGC CCT G-3′
STIM1_gRNA2 rev: 5′-AAA CCA GGG CAA GAC GGA CGC ATA C-3′

The oligo pairs were annealed by incubating for 5 min at 95 °C in a thermocycler and then ramping down to 25 °C at 5 °C/min. The dsDNA guide inserts were ligated into BbsI-digested p × 330.pgkpuro vector [45]. HEK293 cells seeded in a 6-well plate were co-transfected with 1 µg of each plasmid using Lipofectamine® 2000 (Thermo Fisher Scientific) when the cells were 50–60% confluent. The transfectants were subjected to 96 h of puromycin selection (1.5 µg/ml), 24 h after transfection.

For further knockout of Orai1, the guide RNA pairs within exon 2 and exon 3 were identified using the Benchling CRISPR webtool and the following complementary oligos with BbsI compatible overhangs were designed:

Exon 2:
Orai1_gRNA1 for: 5′-CAC CGA TCG GCC AGA GTT ACT CCG-3′
Orai1_gRNA1 rev: 5′-AAA CCG GAG TAA CTC TGG CCG ATC-3′
Exon3:
Orai1_gRNA2 for: 5′-CAC CGG CGG AGT TTG CCC GCT TAC-3′
Orai1_gRNA2 rev: 5′-AAA CGT AAG CGG GCA AAC TCC GCC-3′

The oligo pairs were annealed as mentioned above. The dsDNA guide inserts with BbsI overhangs were ligated into BbsI-digested pU6-(BbsI) CBh-Cas9-T2 A-mCherry (Addgene Plasmid #64324). The resulting constructs were co-transfected in HEK293 STIM1 KO cells seeded in a T25 flask using Lipofectamine 2000. The transfected cells were FACS-sorted with mCherry fluorescence, and single cells were seeded in a 96-well plate. The cells were tested by Ca^{2+} imaging with FURA-2 and a single-cell-derived clone, F4, was functionally confirmed to have undergone knockout of STIM1 and Orai1 (Supp-Fig. 7). Cells were used until passage 18.

4.4. Electrophysiology

Electrophysiological experiments were performed using the patch-clamp technique in whole-cell recording configurations at 21–25 °C. An Ag/AgCl electrode was used as reference electrode. Voltage ramps were applied every 5 s from a holding potential of 0 mV, covering a range of −90 mV to + 90 mV over 1 s. For passive store depletion the internal pipette solution included (in mM): 145 Cs methane sulfonate, 20 EGTA, 10 HEPES, 8 NaCl, 3,5 $MgCl_2$, pH 7.2. Standard extracellular solution consisted of (in mM) 145 NaCl, 10 HEPES, 10 $CaCl_2$, 10 glucose, 5 CsCl, 1 $MgCl_2$, pH 7.4. A liquid junction potential correction of + 12 mV was applied, resulting from a Cl^--based bath solution and a sulfonate-based pipette solution. All currents were leak subtracted either by subtracting the initial voltage ramps obtained shortly following break-in with no visible current activation, or with constitutively active currents after application of 10 µm La^{3+} at the end of the experiment. All experiments were carried out at least on two different days.

4.5. Confocal FRET fluorescence microscopy

Confocal FRET microscopy was performed on HEK293 cells, as previously described [46]. In brief, a QLC100 Real-Time Confocal System (VisiTech Int.) connected to two Photometrics CoolSNAPHQ monochrome cameras (Roper Scientific) and a dual port adapter (dichroic: 505lp; cyan emission filter: 485/30; yellow emission filter: 535/50; Chroma Technology Corp.) was used for recording fluorescence images. This system was attached to an Axiovert 200 M microscope (Zeiss, Germany) in conjunction with two diode lasers (445 nm, 515 nm) (Visitron Systems). Image acquisition and control of the confocal system was performed with a Visiview 2.1.1 software (Visitron Systems). Image correction due to cross-talk and cross-excitation were performed prior to the calculation. Therefore, appropriate cross-talk calibration factors were determined for each construct on each day of the FRET experiment. After threshold determination and background subtraction, the corrected FRET (E_{app}) was calculated on a pixel-to-pixel basis using a custom-made software [46] integrated in MatLab 7.0.4 according to the method published by Zal and Gascoigne [47], with a microscope-specific constant G value of 2.0. All experiments were performed at room temperature. The Pearson correlation coefficient (R-value) was used to measure the strength of the linear association/co-localization between STIM1 and Orai1 variants, where a value R = 1 meant a perfect positive correlation/co-localization.

4.6. Cell preparation, diamide-crosslinking and western blot analysis

HEK293 STIM1/Orai1 double KO cells cultured in 12-cm dishes were transfected with 5 µg plasmid using Transfectin lipid reagent (Biorad) following the manufacturer's instructions. 24 h after transfection, cells were treated with 1 µM TG solution [1 µM TG in 0 mM Ca^{2+} extracellular solution] for 3 min at room temperature. After TG incubation, cells were treated with 1 mM diamide-solution for 5 min at room temperature, and the reaction was stopped upon addition of 50 mM N-ethylmaleimide quenching solution. Cells were then harvested and washed twice in an HBSS (Hank's balanced salt solution) buffer containing 1 mM EDTA. After centrifugation (1000 *g*/2 min), cell pellets were resuspended in homogenization buffer [25 mM Tris HCl pH 7.4, 50 mM NaCl, protease inhibitor (Roche)] and incubated on ice for 15 min. Lysed cells were passed 10 times through a 27 G ½" needle and centrifuged at 1000 *g* for 15 min at 4 °C to pellet debris. 21 µl of each sample were mixed with nonreducing Laemmli's buffer, heated 15 min at 55 °C and subjected to 3–8% Tris-acetate gels (BioRad). For breaking up the disulphide bonds, samples were treated 10 min with BMS. Separated proteins were transferred to a nitrocellulose membrane and immunoblotted with an antibody recognizing STIM1 (Cell signalling technology) or Orai1 (Sigma Aldrich), respectively. Each experiment was performed at least three independent times.

4.7. Statistics

The results are depicted as means ± s.e.m. determined for the indicated number of experiments. For statistical comparison, the Student's two-tailed *t* test was applied. * $p < 0.05$ always in correlation to WT.

Data availability

Data supporting the findings of this manuscript are available from the corresponding authors upon reasonable request.

Author contributions

CB, MM and CR conceived and coordinated the study and wrote the paper. CB, ID, MS and AK performed and analysed electrophysiological experiments. MM and RS carried out fluorescence microscopy experiments. CB, AK and SL performed molecular biology methods. RB and MH generated as well as characterized CRSISPR-Cas9 STIM1/Orai1 double knockout cells, and contributed to the manuscript writing. VL and IF performed and analysed biochemical cysteine crosslinking experiments. KG contributed with data analysis as well as interpretation

and manuscript writing. All authors reviewed the results and approved the final version of the manuscript.

Conflict of interest

The authors declare that they have no conflicts of interest with the contents of this article.

Acknowledgments

We thank S. Buchegger for excellent technical assistance. Further, we thank Dr. Natalia Domanitskaia and Prof. Sven Rottenberg, Institute of Animal Pathology, University of Bern for their guidance in CRISPR/Cas9 knockouts. We would like to thank Dr. Stefan Mueller and Thomas Schaffer at the FACS facility, Institute of Pathology, University of Bern for their help in FACS sorting. Also, we thank Tamara Locher, University of Bern for her technical assistance in cell culture. Michael Stadlbauer has a PhD scholarship of the FWF-PhD program W1250 “NanoCell”. This work was supported by Swiss National Foundation Sinergia grant CRSII3_16078 to M.A.H. Support has been provided by the Austrian Science Fund (FWF) projects P28498 to M.M., P27641 I.D., P27263 C.R, and Austrian BMWFW HSRSM (PromOpt2.0 to K.G. and C.R.).

Appendix A. Supplementary data

Supplementary material related to this article can be found, in the online version, at doi:https://doi.org/10.1016/j.ceca.2019.02.009.

References

[1] A.B. Parekh, J.W. Putney Jr., Store-operated calcium channels, Physiol. Rev. 85 (2005) 757–810.
[2] J. Liou, M.L. Kim, W.D. Heo, J.T. Jones, J.W. Myers, J.E. Ferrell Jr, T. Meyer, STIM is a Ca2+ sensor essential for Ca2+-store-depletion-triggered Ca2+ influx, Curr. Biol. 15 (2005) 1235–1241.
[3] J. Roos, P.J. DiGregorio, A.V. Yeromin, K. Ohlsen, M. Lioudyno, S. Zhang, O. Safrina, J.A. Kozak, S.L. Wagner, M.D. Cahalan, G. Velicelebi, K.A. Stauderman, STIM1, an essential and conserved component of store-operated Ca2+ channel function, J. Cell Biol. 169 (2005) 435–445.
[4] M. Prakriya, S. Feske, Y. Gwack, S. Srikanth, A. Rao, P.G. Hogan, Orai1 is an essential pore subunit of the CRAC channel, Nature 443 (2006) 230–233.
[5] S.L. Zhang, A.V. Yeromin, X.H.F. Zhang, Y. Yu, O. Safrina, A. Penna, J. Roos, K.A. Stauderman, M.D. Cahalan, Genome-wide RNAi screen of Ca2+ influx identifies genes that regulate Ca2+ release-activated Ca2+ channel activity, Proceedings of the National Academy of Sciences %R 103 (2006) 9357–9362, https://doi.org/10.1073/pnas.0603161103.
[6] M. Vig, C. Peinelt, A. Beck, D.L. Koomoa, D. Rabah, M. Koblan-Huberson, S. Kraft, H. Turner, A. Fleig, R. Penner, J.P. Kinet, CRACM1 is a plasma membrane protein essential for store-operated Ca2+ entry, Science 312 (2006) 1220–1223.
[7] P.G. Hogan, R.S. Lewis, A. Rao, Molecular basis of calcium signaling in lymphocytes: STIM and ORAI, Annu. Rev. Immunol. 28 (2010) 491–533.
[8] M. Prakriya, R.S. Lewis, Store-operated calcium channels, Physiol. Rev. 95 (2015) 1383–1436.
[9] I. Grigoriev, S.M. Gouveia, B. van der Vaart, J. Demmers, J.T. Smyth, S. Honnappa, D. Splinter, M.O. Steinmetz, J.W. Putney Jr., C.C. Hoogenraad, A. Akhmanova, STIM1 is a MT-Plus-End-Tracking protein involved in remodeling of the ER, Curr. Biol. 18 (2008) 177–182.
[10] S. Honnappa, S.M. Gouveia, A. Weisbrich, F.F. Damberger, N.S. Bhavesh, H. Jawhari, I. Grigoriev, F.J. van Rijssel, R.M. Buey, A. Lawera, I. Jelesarov, F.K. Winkler, K. Wuthrich, A. Akhmanova, M.O. Steinmetz, An EB1-binding motif acts as a microtubule tip localization signal, Cell 138 (2009) 366–376.
[11] Y. Baba, K. Hayashit, Y. Fujii, A. Mizushima, H. Watarai, M. Wakamori, T. Numaga, Y. Mori, M. Iino, M. Hikida, T. Kurosaki, Coupling of STIM1 to store-operated Ca2+ entry through its constitutive and inducible movement in the endoplasmic reticulum, Proc. Natl. Acad. Sci. U. S. A. 103 (2006) 16704–16709.
[12] J.T. Smyth, W.I. Dehaven, G.S. Bird, J.W. Putney Jr, Ca2+-store-dependent and -independent reversal of Stim1 localization and function, J. Cell. Sci. 121 (2008) 762–772.
[13] J. Soboloff, B.S. Rothberg, M. Madesh, D.L. Gill, STIM proteins: dynamic calcium signal transducers, Nat. Rev. Mol. Cell Biol. 13 (2012) 549–565.
[14] V.A. Barr, K.M. Bernot, S. Srikanth, Y. Gwack, L. Balagopalan, C.K. Regan, D.J. Helman, C.L. Sommers, M. Oh-Hora, A. Rao, L.E. Samelson, Dynamic movement of the calcium sensor STIM1 and the calcium channel Orai1 in activated T-cells: puncta and distal caps, Mol. Biol. Cell 19 (2008) 2802–2817.
[15] M. Muik, I. Frischauf, I. Derler, M. Fahrner, J. Bergsmann, P. Eder, R. Schindl, C. Hesch, B. Polzinger, R. Fritsch, H. Kahr, J. Madl, H. Gruber, K. Groschner, C. Romanin, Dynamic coupling of the putative coiled-coil domain of ORAI1 with STIM1 mediates ORAI1 channel activation, J. Biol. Chem. 283 (2008) 8014–8022.
[16] L. Navarro-Borelly, A. Somasundaram, M. Yamashita, D. Ren, R.J. Miller, M. Prakriya, STIM1-Orai1 interactions and Orai1 conformational changes revealed by live-cell FRET microscopy, J. Physiol. 586 (2008) 5383–5401.
[17] P.G. Hogan, The STIM1-ORAI1 microdomain, Cell Calcium 58 (2015) 357–367.
[18] M. Muik, M. Fahrner, R. Schindl, P. Stathopulos, I. Frischauf, I. Derler, P. Plenk, B. Lackner, K. Groschner, M. Ikura, C. Romanin, STIM1 couples to ORAI1 via an intramolecular transition into an extended conformation, EMBO J. 30 (2011) 1678–1689.
[19] R.M. Luik, B. Wang, M. Prakriya, M.M. Wu, R.S. Lewis, Oligomerization of STIM1 couples ER calcium depletion to CRAC channel activation, Nature 454 (2008) 538–542.
[20] M. Fahrner, M. Muik, R. Schindl, C. Butorac, P. Stathopulos, L. Zheng, I. Jardin, M. Ikura, C. Romanin, A coiled-coil clamp controls both conformation and clustering of stromal interaction molecule 1 (STIM1), J. Biol. Chem. 289 (2014) 33231–33244.
[21] Y. Zhou, P. Meraner, H.T. Kwon, D. Machnes, M. Oh-hora, J. Zimmer, Y. Huang, A. Stura, A. Rao, P.G. Hogan, STIM1 gates the store-operated calcium channel ORAI1 in vitro, Nat. Struct. Mol. Biol. 17 (2010) 112–116.
[22] P.B. Stathopulos, R. Schindl, M. Fahrner, L. Zheng, G.M. Gasmi-Seabrook, M. Muik, C. Romanin, M. Ikura, STIM1/Orai1 coiled-coil interplay in the regulation of store-operated calcium entry, Nat. Commun. 4 (2013) 2963.
[23] R. Palty, E.Y. Isacoff, Cooperative binding of stromal interaction molecule 1 (STIM1) to the N and C termini of calcium release-activated calcium modulator 1 (Orai1), J. Biol. Chem. 291 (2016) 334–341.
[24] I. Derler, P. Plenk, M. Fahrner, M. Muik, I. Jardin, R. Schindl, H.J. Gruber, K. Groschner, C. Romanin, The extended transmembrane Orai1 N-terminal (ETON) region combines binding interface and gate for Orai1 activation by STIM1, J. Biol. Chem. 288 (2013) 29025–29034.
[25] S. Srikanth, H.J. Jung, B. Ribalet, Y. Gwack, The intracellular loop of Orai1 plays a central role in fast inactivation of Ca2+ release-activated Ca2+ channels, J. Biol. Chem. 285 (2010) 5066–5075.
[26] C.Y. Park, P.J. Hoover, F.M. Mullins, P. Bachhawat, E.D. Covington, S. Raunser, T. Walz, K.C. Garcia, R.E. Dolmetsch, R.S. Lewis, STIM1 clusters and activates CRAC channels via direct binding of a cytosolic domain to Orai1, Cell 136 (2009) 876–890.
[27] X. Wang, Y. Wang, Y. Zhou, E. Hendron, S. Mancarella, M.D. Andrake, B.S. Rothberg, J. Soboloff, D.L. Gill, Distinct Orai-coupling domains in STIM1 and STIM2 define the Orai-activating site, Nat. Commun. 5 (2014) 3183.
[28] Z. Li, L. Liu, Y. Deng, W. Ji, W. Du, P. Xu, L. Chen, T. Xu, Graded activation of CRAC channel by binding of different numbers of STIM1 to Orai1 subunits, Cell Res. 21 (2011) 305–315.
[29] J. Liou, M. Fivaz, T. Inoue, T. Meyer, Live-cell imaging reveals sequential oligomerization and local plasma membrane targeting of stromal interaction molecule 1 after Ca2+ store depletion, Proc. Natl. Acad. Sci. U. S. A. 104 (2007) 9301–9306.
[30] C.N. Pace, J.M. Scholtz, A helix propensity scale based on experimental studies of peptides and proteins, Biophys. J. 75 (1998) 422–427.
[31] V. Nesin, G. Wiley, M. Kousi, E.C. Ong, T. Lehmann, D.J. Nicholl, M. Suri, N. Shahrizaila, N. Katsanis, P.M. Gaffney, K.J. Wierenga, L. Tsiokas, Activating mutations in STIM1 and ORAI1 cause overlapping syndromes of tubular myopathy and congenital miosis, Proc. Natl. Acad. Sci. U. S. A. (2014).
[32] D. Misceo, A. Holmgren, W.E. Louch, P.A. Holme, M. Mizobuchi, R.J. Morales, A.M. De Paula, A. Stray-Pedersen, R. Lyle, B. Dalhus, G. Christensen, H. Stormorken, G.E. Tjonnfjord, E. Frengen, A dominant STIM1 mutation causes Stormorken syndrome, Hum. Mutat. 35 (2014) 556–564.
[33] G. Morin, N.O. Bruechle, A.R. Singh, C. Knopp, G. Jedraszak, M. Elbracht, D. Bremond-Gignac, K. Hartmann, H. Sevestre, P. Deutz, D. Herent, P. Nurnberg, B. Romeo, K. Konrad, M. Mathieu-Dramard, J. Oldenburg, E. Bourges-Petit, Y. Shen, K. Zerres, H. Ouadid-Ahidouch, J. Rochette, Gain-of-Function mutation in STIM1 (p.R304W) is associated with Stormorken syndrome, Hum. Mutat. (2014).
[34] M. Fahrner, M. Stadlbauer, M. Muik, P. Rathner, P. Stathopulos, M. Ikura, N. Muller, C. Romanin, A dual mechanism promotes switching of the Stormorken STIM1 R304W mutant into the activated state, Nat. Commun. 9 (2018) 825.
[35] R. Palty, Z. Fu, E.Y. Isacoff, Sequential steps of CRAC channel activation, Cell Rep. 19 (2017) 1929–1939.
[36] Y. Zhou, X. Cai, N.A. Loktionova, X. Wang, R.M. Nwokonko, Y. Wang, B.S. Rothberg, M. Trebak, D.L. Gill, The STIM1-binding site nexus remotely controls Orai1 channel gating, Nat. Commun. 7 (2016) 13725.
[37] B.A. McNally, A. Somasundaram, A. Jairaman, M. Yamashita, M. Prakriya, The C- and N-terminal STIM1 binding sites on Orai1 are required for both trapping and gating CRAC channels, J. Physiol. (2013).
[38] Y. Zhou, X. Cai, R.M. Nwokonko, N.A. Loktionova, Y. Wang, D.L. Gill, The STIM-Orai coupling interface and gating of the Orai1 channel, Cell Calcium (2017).
[39] Y. Zhou, S. Ramachandran, M. Oh-Hora, A. Rao, P.G. Hogan, Pore architecture of the ORAI1 store-operated calcium channel, Proc. Natl. Acad. Sci. U. S. A. 107 (2010) 4896–4901.
[40] A. Rath, C.M. Deber, Correction factors for membrane protein molecular weight readouts on sodium dodecyl sulfate-polyacrylamide gel electrophoresis, Anal. Biochem. 434 (2013) 67–72.
[41] X. Hou, L. Pedi, M.M. Diver, S.B. Long, Crystal structure of the calcium release-activated calcium channel Orai, Science (2012).
[42] M. Fahrner, S.K. Pandey, M. Muik, L. Traxler, C. Butorac, M. Stadlbauer, V. Zayats, A. Krizova, P. Plenk, I. Frischauf, R. Schindl, H.J. Gruber, P. Hinterdorfer, R. Ettrich, C. Romanin, I. Derler, Communication between N terminus and loop2 tunes Orai

activation, J. Biol. Chem. 293 (2018) 1271–1285.
[43] I. Frischauf, M. Litvinukova, R. Schober, V. Zayats, B. Svobodova, D. Bonhenry, V. Lunz, S. Cappello, L. Tociu, D. Reha, A. Stallinger, A. Hochreiter, T. Pammer, C. Butorac, M. Muik, K. Groschner, I. Bogeski, R.H. Ettrich, C. Romanin, R. Schindl, Transmembrane helix connectivity in Orai1 controls two gates for calcium-dependent transcription, Sci. Signal. 10 (2017).
[44] X. Hou, S.R. Burstein, S. Long, (2018).
[45] T. Harmsen, S. Klaasen, H. van de Vrugt, H. Te Riele, DNA mismatch repair and oligonucleotide end-protection promote base-pair substitution distal from a CRISPR/Cas9-induced DNA break, Nucleic Acids Res. (2018).
[46] I. Derler, M. Hofbauer, H. Kahr, R. Fritsch, M. Muik, K. Kepplinger, M.E. Hack, S. Moritz, R. Schindl, K. Groschner, C. Romanin, Dynamic but not constitutive association of calmodulin with rat TRPV6 channels enables fine tuning of Ca2+-dependent inactivation, J. Physiol. 577 (2006) 31–44.
[47] T. Zal, N.R. Gascoigne, Photobleaching-corrected FRET efficiency imaging of live cells, Biophys. J. 86 (2004) 3923–3939.